

See discussions, stats, and author profiles for this publication at: <https://www.researchgate.net/publication/239727836>

The molecular structure of gaseous dimethylamidogallane: Characterization of the dimer $[\text{Me}_2\text{NGaH}_2]_2$ by electron diffraction and vibrational spectroscopy

ARTICLE in JOURNAL OF THE CHEMICAL SOCIETY DALTON TRANSACTIONS · JANUARY 1985

Impact Factor: 4.1 · DOI: 10.1039/dt9850000807

CITATIONS

44

READS

3

4 AUTHORS, INCLUDING:



Anthony J Downs

University of Oxford

258 PUBLICATIONS 5,007 CITATIONS

SEE PROFILE

The Molecular Structure of Gaseous Dimethylamidogallane: Characterization of the Dimer $[\text{Me}_2\text{NGaH}_2]_2$ by Electron Diffraction and Vibrational Spectroscopy†

Paul L. Baxter and Anthony J. Downs*

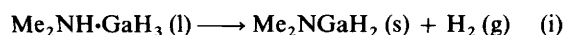
Department of Inorganic Chemistry, University of Oxford, South Parks Road, Oxford OX1 3QR

David W. H. Rankin* and Heather E. Robertson

Department of Chemistry, University of Edinburgh, West Mains Road, Edinburgh EH9 3JJ

The structure of gaseous dimethylamidogallane has been determined by electron diffraction. The predominant species is shown to be not the monomer Me_2NGaH_2 , as suggested previously, but the dimer $[\text{Me}_2\text{NGaH}_2]_2$ with a cyclic Ga_2N_2 skeleton and effective symmetry D_{2h} . Salient structural parameters (r_s) are: $r(\text{Ga}-\text{N})$ 202.7(0.4), $r(\text{Ga}-\text{H})$ 148.7(3.6), and $r(\text{N}-\text{C})$ 146.3(1.3) pm; $\text{Ga}-\text{N}-\text{Ga}$ 90.6(0.8) and $\text{C}-\text{N}-\text{C}$ 109.6(1.6)°. The vibrational spectra of the compound, with either hydrogen or deuterium linked to the gallium, indicate that the dimeric unit is retained in benzene solution and in the crystalline state and have been analysed accordingly.

Dimethylamidogallane is a white crystalline solid formed quantitatively at room temperature by the slow elimination of hydrogen from dimethylamine-gallane [equation (i)].^{1,2} The



compound is reported to resemble the corresponding borane³ in being dimeric in benzene solution; the corresponding alane is trimeric under these conditions.⁴ On the basis of its i.r. spectrum, however, the vapour of the gallane has been judged to consist predominantly of the monomer Me_2NGaH_2 .² If this is correct, the molecule is unique in being a low-temperature derivative of gallane with a three-co-ordinate metal atom, and its structure invites comparison with that we have recently determined by electron diffraction for $\text{Me}_3\text{N}\cdot\text{GaH}_3$.⁵ Of particular interest are the lengths of the $\text{Ga}-\text{N}$ bonds since monomeric dimethylamidogallane can be formulated as $\text{Me}_2\text{N} \Rightarrow \text{GaH}_2$ with a degree of multiple bonding between the gallium and nitrogen atoms. In this context, it is noteworthy that the i.r. spectrum of gaseous dimethylamidogallane has been interpreted in terms of a $\text{Ga}-\text{N}$ stretching mode with an energy (743 cm^{-1}) markedly higher than that (527 cm^{-1}) of the analogous mode of trimethylamine-gallane.^{2,6,7}

The attention attracted currently by compounds in which the heavier typical elements engage in multiple bonding⁸ has combined with our more specific interest in the structural and chemical properties of molecules containing $\text{Ga}-\text{H}$ bonds to prompt a structural investigation of gaseous dimethylamidogallane by electron diffraction. In addition, we have extended earlier investigations of the vibrational spectra² to include not only the vapour but also the solid and benzene solutions of the isotopomers $[\text{Me}_2\text{NGaH}_2]_x$ and $[\text{Me}_2\text{NGaD}_2]_x$. The electron diffraction pattern leaves little doubt that the compound vaporises predominantly not as the monomer ($x = 1$) but as the dimer ($x = 2$). Both the electron scattering and the i.r. spectra can be interpreted satisfactorily on the basis of a model with a four-membered Ga_2N_2 ring and complying effectively with D_{2h} symmetry. Indeed the vibrational spectra suggest that the same molecule is present in benzene solution and in the crystalline solid.

Experimental

Synthesis.—Dimethylamidogallane was prepared largely in accordance with the procedure described previously² and man-

Table 1. Nozzle-to-plate distances, weighting functions, correlation parameters, scale factors, and electron wavelengths

Nozzle-to-plate distance/mm	Δs	$s_{\text{min.}}$	sw_1	sw_2	$s_{\text{max.}}$	Correlation, p/h	Scale factor, k^a	Electron wavelength ^b /pm
285.7	2	20	40	120	144	0.2862	0.697(9)	5.684
128.4	4	60	80	250	300	0.0862	0.283(12)	5.697

^a Figures in parentheses are the estimated standard deviations of the last digits. ^b Determined by reference to the scattering pattern of benzene vapour.

ipulated using conventional vacuum-line techniques. Gallium(III) chloride was prepared by the direct interaction of gallium (Alcoa Chemicals) and chlorine, and lithium tetrahydrogallate or tetra-deuteriogallate by the reaction of lithium hydride or deuteride (Aldrich Chemicals) with gallium(III) chloride in diethyl ether.⁹ The reaction of $\text{Li}[\text{GaH}_4]$ or $\text{Li}[\text{GaD}_4]$ with dimethylammonium chloride (Aldrich Chemicals) in diethyl ether provided the source of $\text{Me}_2\text{NH}\cdot\text{GaH}_3$ or $\text{Me}_2\text{NH}\cdot\text{GaD}_3$; after purification by vacuum distillation, this was left stored *in vacuo* at room temperature for 14 d to bring about the formation of dimethylamidogallane in accordance with equation (i). The amido-derivative was in turn purified by vacuum sublimation and its purity checked by reference to the i.r. spectrum of the vapour.

Electron-diffraction Measurements.—Electron-scattering patterns were recorded photographically on Kodak Electron Image plates using the Edinburgh gas-diffraction apparatus.¹⁰ The sample was held at ambient temperature (corresponding to an equilibrium vapour pressure of ca. 1 mmHg²) in an ampoule closed by a greased stopcock and gained access to the nozzle of the diffraction apparatus *via* a greased glass taper joint and a stainless-steel needle valve. The plates were left in air for 16 h before developing in an effort to reduce the effects of reaction between the vapour and the emulsion. Despite this, some fogging was unavoidable, especially with the shorter nozzle-to-plate distance which entailed longer exposure times. The nozzle-to-plate distances and electron wavelengths are given in Table 1, together with the weighting functions used to set up the off-diagonal weight matrix, the correlation parameters, and final scale factors.

Details of the electron-scattering patterns were collected in digital form using a Joyce-Loebl MDM6 microdensitometer.¹¹

† Non-S.I. units employed: mmHg = (101 325/760) N m⁻², a.m.u. = 1.6605 × 10⁻²⁷ kg.

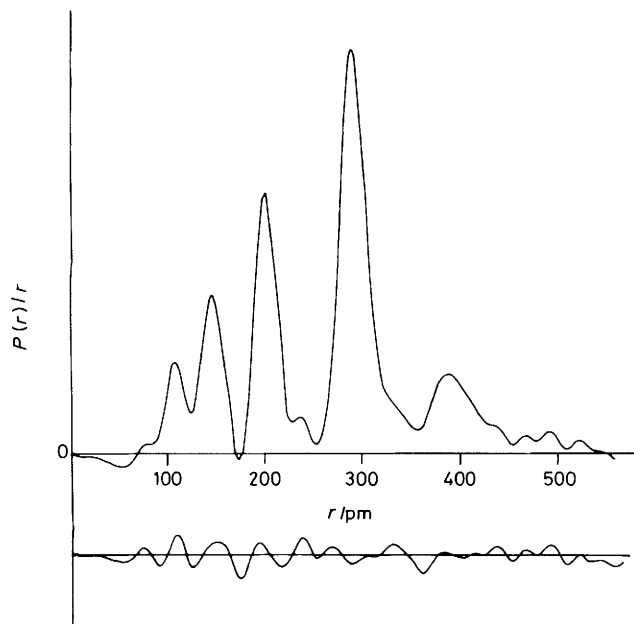


Figure 1. Observed and difference radial-distribution curves, $P(r)/r$ versus r , for dimethylamidogallane. Before Fourier inversion the data were multiplied by $s \cdot \exp[(-0.000\ 035\ s^2)/(Z_{Ga} - f_{Ga})(Z_N - f_N)]$

Calculations, performed on an ICL 2970 computer at the Edinburgh Regional Computing Centre, were accomplished with the programs for data reduction¹¹ and least-squares refinement¹² described elsewhere, the complex scattering factors being those listed by Schäfer *et al.*¹³

Vibrational Spectroscopy.—I.r. spectra of gaseous or solid samples of $[\text{Me}_2\text{NGaH}_2]_x$ or $[\text{Me}_2\text{NGaD}_2]_x$ were measured with a Pye-Unicam model SP 2000 or Perkin-Elmer model 580A spectrophotometer. Raman spectra of solid samples or solutions, measured with a Spex Ramalog 5 spectrophotometer, were excited at $\lambda = 514.5\text{ nm}$ using the output from a Spectra-Physics model 165 Ar^+ laser. The vapour was contained in a Pyrex-bodied cell having a pathlength of 10 cm and fitted with CsI windows. Solid films of the gallane were formed by condensation of the vapour on a CsI window (for i.r. studies) or a copper block (for Raman studies) supported in an evacuated glass shroud and held at 77 K. After annealing, the condensate was recooled to 77 K before its spectrum was recorded. A benzene solution *ca.* 0.2 mol dm^{-3} in the gallane was contained in a thin-walled Pyrex capillary and held at room temperature while its Raman spectrum was measured.

Results and Discussion

Structure of the Gaseous Molecule.—On the evidence of the positions, relative intensities, and number of bands in the i.r. spectrum, Greenwood *et al.*² deduced that gaseous dimethylamidogallane consists of monomeric Me_2NGaH_2 molecules in which the C_2NGaH_2 skeleton conforms to C_{2v} symmetry. However, we have been unable to accommodate such a model on the basis of the measured electron scattering displayed by the vapour, failing to find any solution with $R_G < 0.4$. Figure 1 depicts the radial-distribution curve, $P(r)/r$ vs. r , derived from the experimental data sets after scaling, combination, and Fourier transformation. We note in particular the appearance of considerable scattering intensity corresponding to interatomic distances greater than 350 pm, a feature quite

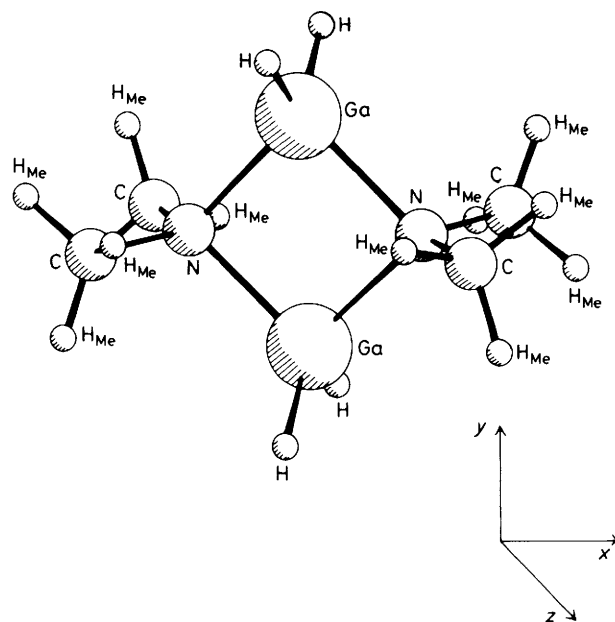


Figure 2. Perspective view of the molecule $[\text{Me}_2\text{NGaH}_2]_2$

incompatible with the scattering properties expected of monomeric Me_2NGaH_2 .

In place of the monomeric unit we have therefore adopted for our structural model a dimer, $[\text{Me}_2\text{NGaH}_2]_2$, with the dimethylamido-groups providing symmetrical bridges between the gallium atoms to generate a planar Ga_2N_2 ring and a $[\text{C}_2\text{NGaH}_2]_2$ skeleton with D_{2h} symmetry. As indicated in the following section, this is consistent with the vibrational spectra of the compound. We note too that analogous structures centred on a planar four-membered ring have been deduced by spectroscopic and diffraction methods for the compounds $[\text{Me}_2\text{NBX}_2]_2$ ($X = \text{F}^{14}$ or Cl^{15}), $[\text{Me}_2\text{NAlMe}_2]_2$,¹⁶ $[\text{Me}_2\text{-NAlCl}_2]_2$,¹⁷ and $[\text{Me}_2\text{NInMe}_2]_2$.¹⁸ The model we have chosen for $[\text{Me}_2\text{NGaH}_2]_2$ involves nine independent geometrical parameters. With reference to the perspective view of the molecule shown in Figure 2, these comprise the four bonded distances Ga–N, Ga–H, N–C, and C–H_{Me}, and the five angles Ga–N–Ga, C–N–C, N–C–H_{Me}, H–Ga–H, and θ defining the twisting of each methyl group about the N–C bond (away from the configuration in which the whole molecule possesses D_{2h} symmetry).

Molecular-scattering intensities have been calculated by established procedures and the molecular structure has been refined on this basis by full-matrix least-squares analysis. We have not applied shrinkage corrections in our refinements but have no reason to suppose that this will make any significant difference to the molecular parameters we have derived. Estimated standard deviations take into account the effects of correlation, whether involving data points or the molecular parameters themselves, and have been increased to allow for systematic errors in the electron wavelength, nozzle-to-plate distance, *etc.*

On the basis of a dimeric model we are able qualitatively to account for the principal features of the radial-distribution curve (Figure 1). Thus, the most prominent peak located at *ca.* 295 pm arises primarily from scattering by the eight equivalent non-bonded $\text{Ga} \cdots \text{C}$ distances. The bonded Ga–N atom pairs account for most of the scattering near 200 pm while a shoulder at *ca.* 290 pm on the flank of the large $\text{Ga} \cdots \text{C}$ peak is associated with the $\text{Ga} \cdots \text{Ga}$ distance. Scattering from the

Table 2. Least-squares correlation matrix ($\times 100$)* for the molecule dimethylamidogallane

Distances				Angles		Vibrational amplitudes				Scale factors		
r_1	r_2	r_3	r_4	GaNGa	CNC	u_1	u_5	u_6	u_8	k_1	k_2	
100	8	-21	-23	-19	50	2	11	-4	-3	-8	-9	r_1
	100	-83	25	47	-34	-24	30	6	-46	5	2	r_2
		100	4	-48	45	13	-34	-11	34	-1	-1	r_3
			100	16	1	-22	3	-2	-16	6	-1	r_4
				100	-7	2	79	-32	-19	28	7	GaNGa
					100	13	10	-11	13	3	-5	CNC
						100	14	11	19	37	39	u_1
							100	-57	-8	46	14	u_5
								100	0	-8	20	u_6
									100	10	3	u_8
										100	30	k_1
											100	k_2

* Numbers in bold type indicate marked correlation.

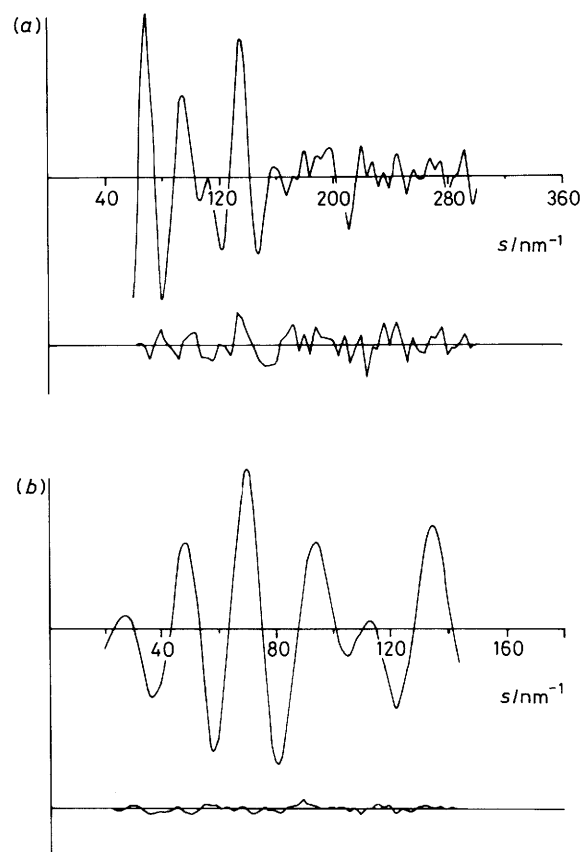
Table 3. The molecular parameters^a for dimethylamidogallane, $[\text{Me}_2\text{NGaH}_2]_2$

Parameter	Distance/pm or angle/°		Amplitude/pm
(a) Independent distances and amplitudes			
$r_1(\text{Ga-N})$	202.7(0.4)	u_1	4.5(0.9)
$r_2(\text{Ga-H})$	148.7(3.6)		8.0 ^b
$r_3(\text{N-C})$	146.3(1.3)		4.5 ^b
$r_4(\text{C-H}_{\text{Me}})$	107.1(1.3)		6.5 ^b
(b) Dependent distances and amplitudes ^c			
$d_5(\text{Ga} \cdots \text{C})$	294.1(1.2)	u_5	9.2(1.3)
$d_6(\text{N} \cdots \text{N})$	285.2(1.9)		
$d_7(\text{Ga} \cdots \text{Ga})$	288.1(1.7)	u_6	5.7(1.2)
$d_8(\text{Ga} \cdots \text{H}_{\text{Me}})$	388.2(1.7)		
$d_9(\text{Ga} \cdots \text{H}_{\text{Me}})$	383.1(1.6)	u_8	17.7(2.1)
$d_{10}(\text{C} \cdots \text{N})$	388.4(2.3)		
$d_{11}(\text{Ga} \cdots \text{H})$	393.5(4.0)		
(c) Independent angles			
Ga-N-Ga	90.6(0.8)		
C-N-C	109.6(1.6)		
H-C-N	109 ^b		
H-Ga-H	109 ^b		
θ, CH ₃ twisting	20 ^b		

^a Figures in parentheses are the estimated standard deviations of the last digits. ^b Fixed. ^c Other non-bonded distances were included in the refinement, but are not listed here.

bonded Ga-H and C-N atom pairs gives rise to the conspicuous peak at ca. 150 pm, and scattering from the bonded C-H_{Me} atom pairs to the peak at ca. 110 pm. Between 350 and 450 pm there is a broad feature representing mainly the scattering from the following non-bonded atom pairs: C \cdots H_{Me}, Ga \cdots H, C \cdots H, and C \cdots N. Moreover, there are various weak components identifiable with scattering from other non-bonded atom pairs, e.g. N \cdots H_{Me}, C \cdots C, and H \cdots H.

Six of the nine independent geometrical parameters used to define the model are amenable to simultaneous refinement. These are the distances Ga-N, Ga-H, C-N, and C-H_{Me}, and the angles Ga-N-Ga and C-N-C. Independent refinement is also possible for two amplitudes of vibration; these relate to the Ga-N and Ga \cdots C distances. In addition, we have refined as a single parameter the amplitudes of vibration associated with each of the following sets of distances: (i) N \cdots N and Ga \cdots Ga and (ii) Ga \cdots H, C \cdots N, and the two longest

**Figure 3.** Experimental and final-difference molecular-scattering intensities for $[\text{Me}_2\text{NGaH}_2]_2$; nozzle-to-plate distances (a) 128.4 and (b) 285.7 mm

Ga \cdots H_{Me} distances. The angle θ defining the mutual orientation of the CH_3 and NCGa_2 groups has been fixed at 20° following a series of calculations to explore its influence on the R factor. The H-Ga-H angle has been fixed at 109° following similar calculations but we do not attach undue significance to this value as there is very little variation in the R factor and in the values of the other parameters as the angle is varied in the range 109 – 120° .

It has not been possible, because of the background noise resulting from the reaction of the vapour with the photographic

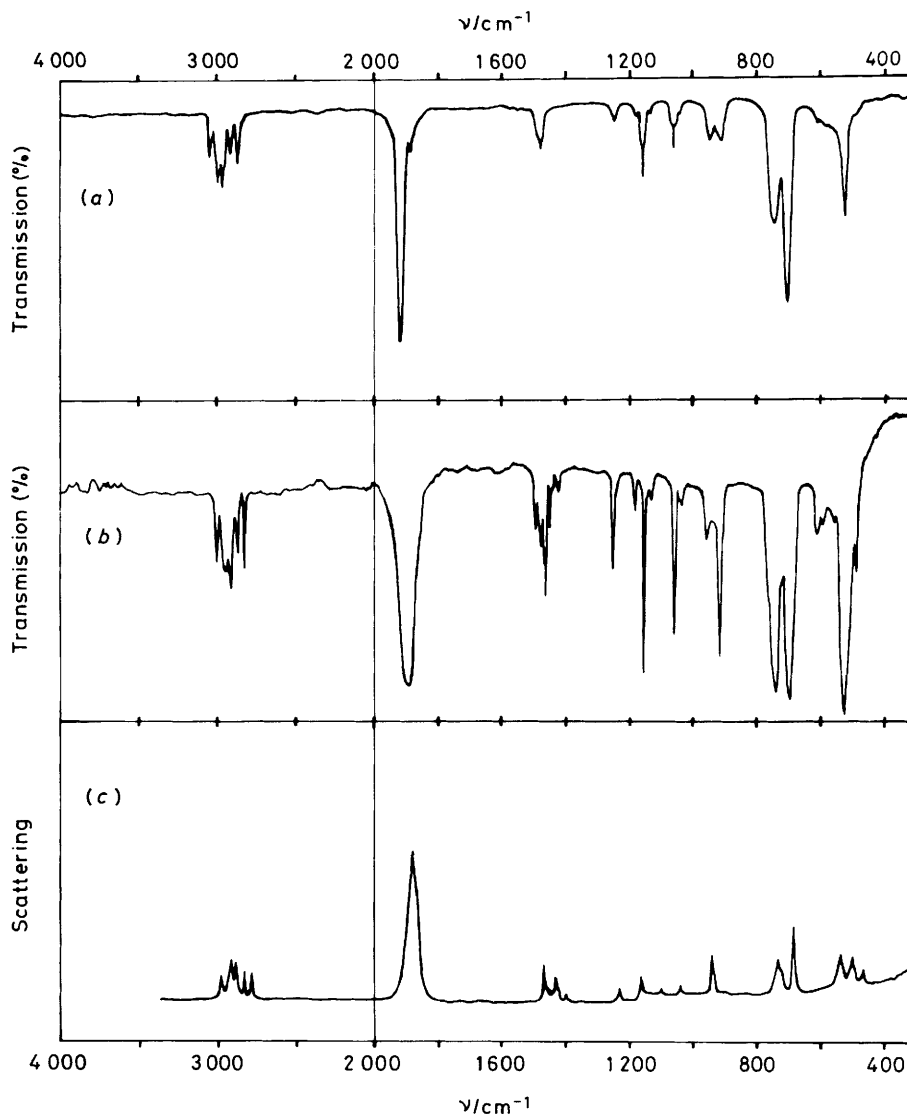


Figure 4. Vibrational spectra of dimethylamidogallane: (a) i.r. spectrum of the vapour at ca. 290 K (pressure ca. 1 mmHg, pathlength 10 cm); (b) i.r. spectrum of an annealed solid film at 77 K; and (c) Raman spectrum of an annealed solid film at 77 K

emulsion, to refine any amplitudes of vibration other than those already detailed. Accordingly we have drawn on the electron-diffraction or spectroscopic precedents set by related molecules to fix reasonable values for the remaining amplitudes.

The final least-squares correlation matrix shows only one major problem of correlation; this involves the N–C and Ga–H bonded distances which are very similar in magnitude (see Table 2). Accordingly the Ga–H distance is relatively poorly defined, as shown by the estimated standard deviation. The success of the refinement may be judged overall by reference to the difference between the experimental radial-distribution curve and that calculated on the basis of the optimum model (Figure 1). Figure 3 offers a similar comparison between the experimental and calculated molecular scattering. The structural details and vibrational amplitudes of the optimum refinement, corresponding to $R_G = 0.121$ ($R_D = 0.091$), are listed in Table 3.

Vibrational Spectra.—Details of the vibrational spectra of dimethylamidogallane with either hydrogen or deuterium bound to the gallium are contained in Table 4, and representative spectra are illustrated in Figure 4. The results relate to the

compound in the vapour or the solid state or in benzene solution where the solute is predominantly dimeric (as judged by the molecular-weight measurements reported previously²). We differ from Greenwood *et al.*² in concluding that the dimeric structure persists in the gaseous as well as the condensed phases, and have analysed the vibrational spectra accordingly in terms of the group vibrations appropriate to the molecule $[\text{Me}_2\text{NGaH}_2]_2$.

Each of the assignments proposed is based on one or more of the following criteria: (a) analogy with the vibrational assignments favoured for other molecules containing a GaH_2 ,^{1,2,19} GeH_2 ,²⁰ or NMe_2 ^{21–25} group or a four-membered M_2N_2 ring ($\text{M} = \text{Al}$,²⁶ Ga ,²⁶ or In ¹⁸); (b) the selection rules expected to govern the i.r. or Raman activity of the vibrational modes associated with the $[\text{Me}_2\text{NGaH}_2]_2$ molecule; (c) the polarization properties of the Raman scattering exhibited by a benzene solution of the gallane; (d) the effect of deuteration at the GaH_2 group on the wavenumber of a given spectroscopic feature, as well as recourse to the product rule as applied to the fundamentals of the $[\text{C}_2\text{NGaH}_2]_2$ and $[\text{C}_2\text{NGaD}_2]_2$ skeletons belonging to a given symmetry class; and (e) the nature of the

Table 4. Vibrational wavenumbers (cm^{-1}) of the isotopomers $[\text{Me}_2\text{NGaH}_2]_2$ and $[\text{Me}_2\text{NGaD}_2]_2$

I.r., vapour, 290 K			I.r., solid, 77 K			Assignment	Raman, solid, 77 K			Raman, C_6H_6 solution, 290 K ^a		
$[\text{Me}_2\text{NGaH}_2]_2$	$[\text{Me}_2\text{NGaD}_2]_2$	$\nu_{\text{H}}/\nu_{\text{D}}$	$[\text{Me}_2\text{NGaH}_2]_2$	$[\text{Me}_2\text{NGaD}_2]_2$	$\nu_{\text{H}}/\nu_{\text{D}}$		$[\text{Me}_2\text{NGaH}_2]_2$	$[\text{Me}_2\text{NGaD}_2]_2$	$\nu_{\text{H}}/\nu_{\text{D}}$	$[\text{Me}_2\text{NGaH}_2]_2$	$[\text{Me}_2\text{NGaD}_2]_2$	$\nu_{\text{H}}/\nu_{\text{D}}$
2 985w 2 930m	2 985m 2 930m	1.00 1.00	2 965m 2 915m	2 975m 2 915m	1.00 1.00	$\nu(\text{C-H})$ + $2 \times \delta(\text{CH}_3)$	2 980m 2 931(sh) 2 923m 2 893m 2 846m 2 799m	2 986m	1.00			
2 905m 2 860w 2 815m	2 905m 2 860m 2 815m	1.00 1.00 1.00	2 880m 2 830m 2 790m	2 885m 2 840m 2 795m	1.00 1.00 1.00			2 926m,br 2 891m 2 843m 2 799m	1.00 1.00 1.00 1.00	b	b	
1 911(sh) 1 907vs 1 901vs	1 378vs 1 371vs 1 355(sh)	1.39	1 885s,br	1 361s	1.39	Symmetric $\nu(\text{Ga-H})$ Antisymmetric $\nu(\text{Ga-H})$	1 890s	1 345s	1.41	1 888vs(p)	1 353vs(p)	1.40
1 870(sh) 1 471w 1 465w	1 466w	1.00	1 476m 1 459m 1 450m 1 443m 1 430m 1 408m	1 470(sh) 1 460m 1 456m 1 435w	1.00 1.00 1.00 1.00		1 875s 1 478m 1 458w,br 1 442w 1 438(sh) 1 408w	1 478m 1 440m,br	1.00 1.00	1 475m 1 447w 1 437(sh)	1 475m 1 447w 1 437(sh)	1.00 1.00
1 234vw	1 235w	1.00	1 233m	1 238w	1.00	$\rho(\text{CH}_3)$	1 239w	1 230w	1.01			
1 167w 1 142w 1 118w	1 170w 1 148m 1 127(sh)	1.00 0.99 0.99	1 168w 1 137s 1 118w	1 164w 1 137m 1 118m	1.00 1.00 1.00		1 166w 1 125vw 1 103vw	1 176w 1 120vw 1 106vw	0.99 1.00 1.00			
1 053m,R 1 047m,Q 1 042m,P	1 053m,R 1 047m,Q 1 042m,P	1.00	1 040s	1 040w	1.00	Antisymmetric $\nu(\text{N-C})$ $2 \times \nu(\text{Ga-N})$ or $\rho(\text{CH}_3)$ sym. $\nu(\text{N-C})$ + $\rho(\text{CH}_3)$?	1 042w	1 030w	1.01			
1 030w 934w 901w	981vw 925m 898(sh)	1.05 1.01 1.00	1 025w 947m 902s	1 025m 925m 896s	1.00 1.02 1.01		942m	908m	1.04	911w	902w 862m	1.01
733m	540m	1.36	725s	520(sh)	1.39	GaH ₂ scissoring + GaH ₂ twisting GaH ₂ wagging $2 \times \delta(\text{NC}_2)$? $\rho(\text{GaH}_2)$ $\nu(\text{Ga-N})$?	734m 725m 686m	617m	1.37 1.36 1.41	752m 742m 686m(dp)	538m 498w	1.40 1.38 1.38
692s 601w 575w 512m 477w	510s 412w c c	1.36 1.40	680s 604w 580w 509s 479m	499s 604w 408w c 475(sh)	1.36 1.00 1.42 1.01		538m 499m 466w	401m 491m 448w 348w	1.34 1.02 1.04 1.00	538w 498w 458w	498w	1.00
281w	281w	1.00	294m			NC ₂ scissoring + NC ₂ wagging $\rho(\text{NC}_2)$? ?	300s d	300m 264m d	1.00	305m(dp) 268s(p) 201m(dp)	301m(dp) 262s(p) d	1.01 1.02

w = Weak, m = medium, s = strong, v = very, sh = shoulder, br = broad, p = polarized, and dp = depolarized. ^a Scattering due to benzene not listed. ^b Region obscured by scattering due to benzene. ^c Obscured by absorption due to $\delta(\text{GaD}_2)$. ^d Obscured by proximity to the Rayleigh line.

Table 5. Proposed assignment of the vibrational fundamentals associated with the $[\text{C}_2\text{NGaH}_2]_2$ skeleton of dimethylamidogallane^a

Symmetry class	Activity ^b	Approximate description of mode	$[\text{Me}_2\text{NGaH}_2]_2$	$[\text{Me}_2\text{NGaD}_2]_2$	$\nu_{\text{H}}/\nu_{\text{D}}^c$
a_g	R(p)	ν_1 symmetric Ga-H stretching	1 888	1 353	1.395
		ν_2 symmetric N-C stretching	911	902	1.010
		ν_3 GaH ₂ scissoring	742	538	1.379
		ν_4 Ga ₂ N ₂ stretching	498	498	1.000
		ν_5 NC ₂ scissoring	268	262	1.023
		ν_6 in-plane Ga ₂ N ₂ deformation	—	—	(1.000)
		ν_7 GaH ₂ torsion	—	—	(1.000)
a_u		ν_8 NC ₂ torsion	—	—	(1.000)
b_{1g}	R(dp)	ν_9 GaH ₂ wagging	686	498	1.378
		ν_{10} Ga ₂ N ₂ stretching	466 ^d	448 ^d	1.040
		ν_{11} NC ₂ rocking	201	—	(1.000)
b_{1u}	I.r.	ν_{12} antisymmetric Ga-H stretching	1 870	1 355	1.380
		ν_{13} antisymmetric N-C stretching	1 047	1 047	1.000
		ν_{14} GaH ₂ rocking	575	412	1.396
		ν_{15} NC ₂ wagging	281	281	1.000
		ν_{16} out-of-plane Ga ₂ N ₂ deformation	—	—	(1.000)
		ν_{17} antisymmetric Ga-H stretching	1 875 ^d	1 345 ^d	1.394
		ν_{18} GaH ₂ rocking	538 ^d	401 ^d	1.342
b_{2g}	R(dp)	ν_{19} NC ₂ twisting	—	—	(1.000)
		ν_{20} symmetric N-C stretching	934	925	1.010
		ν_{21} GaH ₂ wagging	692	510	1.357
b_{2u}	I.r.	ν_{22} Ga ₂ N ₂ stretching	512	—	(1.000)
		ν_{23} NC ₂ scissoring	281	281	1.000
		ν_{24} antisymmetric N-C stretching	1 042 ^d	1 030 ^d	1.012
		ν_{25} GaH ₂ twisting	752	538	1.398
		ν_{26} NC ₂ wagging	300 ^d	300 ^d	1.000
		ν_{27} symmetric Ga-H stretching	1 907	1 371	1.391
		ν_{28} GaH ₂ scissoring	733	540	1.357
b_{3g}	R(dp)	ν_{29} Ga ₂ N ₂ stretching	479 ^d	475 ^d	1.008
		ν_{30} NC ₂ rocking	—	—	(1.000)

^a Assignments refer to a skeleton assumed to have D_{2h} symmetry. The wavenumber of each Raman-active mode is taken from the spectrum of a benzene solution, that of each i.r.-active mode from the spectrum of the vapour. ^b R = Raman-active, i.r. = i.r.-active, p = polarized, and dp = depolarized. ^c Assumed values are given in parentheses. ^d Wavenumber taken from the spectrum of the solid.

envelope associated with a given i.r. absorption of the vapour with its implications for the direction in which the dipole moment oscillates with respect to the molecular framework.

Certain i.r. and Raman bands are readily identified with internal vibrations of the methyl groups forming part of the dimethylamido-ligands, for example by analogy with the vibrational analyses carried out on related molecules, e.g. $[\text{Me}_2\text{NGaMe}_2]_2$,²⁶ $[\text{Me}_2\text{NInMe}_2]_2$,¹⁸ and $\text{E}(\text{NMe}_2)_3$ (E = P or As).²⁵ These occur in the following regions (cm^{-1}): 2 800—3 000, C-H stretching; 1 400—1 480, antisymmetric CH_3 deformation; 1 160—1 240, symmetric CH_3 deformation; and 1 030—1 140, CH_3 rocking modes; there are no features obviously attributable to the CH_3 torsional modes. The positions of the individual bands are virtually invariant, irrespective of the physical state of the compound and of whether the gallium atom is bound to hydrogen or deuterium. Hence it is reasonable to assume that most of the remaining features in the spectra can be meaningfully interpreted in terms of the fundamentals of the D_{2h} skeleton $[\text{C}_2\text{NGaH}_2]_2$; this is the basis of the assignments given in Tables 4 and 5. The descriptions of the normal modes thus employed appear at least to be self-consistent, although how closely they represent the true picture it is impossible to say in the absence of a detailed normal co-ordinate analysis. However, it may be noted that a molecule of the general type XNMe_2 is likely to show extensive mixing of its vibrational fundamentals, especially those involving CH_3 rocking and N-X stretching, as the mass of the substituent X increases.²²

The 30 vibrational modes of the $[\text{C}_2\text{NGaH}_2]_2$ moiety are accommodated by the representation $6a_g + 2a_u + 3b_{1g} +$

Table 6. Moments of inertia, envelopes of vapour-phase i.r. absorptions, and product-rule calculations for the $[\text{C}_2\text{NGaH}_2]_2$ skeleton of dimethylamidogallane

Property	Value
$10^{-6} I_{\text{A}}/\text{a.m.u. pm}^2$	4.3836
$10^{-6} I_{\text{B}}/\text{a.m.u. pm}^2$	4.8415
$10^{-6} I_{\text{C}}/\text{a.m.u. pm}^2$	6.9784
Symmetry parameter $k = (2B - A - C)/(A - C)^a$	0.492
Symmetry parameter $\rho^* = (A - C)/B^a$	0.411
$\tilde{B} + A\tilde{B}/(A + B)/\text{cm}^{-1\text{a}}$	0.0182 6
$\tilde{\beta} = C/2\tilde{B} - 1^a$	-0.3390
$S(\tilde{\beta})^a$	1.4668
$\Delta\nu(\text{PR})/\text{cm}^{-1}$, calculated for type-C band	11.3
$\Delta\nu(\text{PR})/\text{cm}^{-1}$, calculated for type-A or type-B band	9.0

Symmetry class	Product-rule factor ^b	
	Calc.	Obs. ^c
a_g	2.000	1.988
b_{1g}	1.372	1.433
b_{1u}	1.982	1.926
b_{2g}	1.970	1.870
b_{2u}	1.401	1.370
b_{3g}	1.406	1.414
b_{3u}	1.982	1.904

^a See ref. 27: $A = h/8\pi^2 c I_{\text{A}}$, etc.; $\log_{10} S(\tilde{\beta}) = 0.721/(\tilde{\beta} + 4)^{1.13}$. ^b Factor, $P = \nu_i(\text{H}) \cdot \nu_j(\text{H}) \cdots / \nu_i(\text{D}) \cdot \nu_j(\text{D}) \cdots$. ^c Based on the results listed in Table 5.

$5b_{1u} + 3b_{2g} + 4b_{2u} + 3b_{3g} + 4b_{3u}$. Of these 13 ($b_{1u} + b_{2u} + b_{3u}$) are active only in i.r. absorption, 15 ($a_g + b_{1g} + b_{2g} + b_{3g}$) are active only in Raman scattering, and two (a_u) are silent in both spectra. Although the i.r. and Raman spectra should formally comply with the mutual-exclusion rule, in-phase and out-of-phase versions of vibrations involving the NC_2 and GaH_2 groups are likely to have very similar energies resulting in apparent coincidences between features in the i.r. and Raman spectra. Using the dimensions deduced from the electron-diffraction pattern of the vapour, we have calculated the principal moments of inertia of the molecule $[\text{Me}_2\text{NGaH}_2]_2$, with the results collected in Table 6. Formally the molecule is an 'asymmetric top' but it approximates to an oblate 'symmetric top' with the Ga_2N_2 plane containing the axes of I_A and I_B and perpendicular to the axis of I_C , where $I_A \lesssim I_B < I_C$. With the choice of co-ordinate axes shown in Figure 2, the form of the momental ellipsoid is such that b_{1u} modes of the gaseous molecule give rise to type-C, b_{2u} modes to type-A, and b_{3u} modes to type-B i.r. bands. A type-C band is expected to be relatively distinctive with a prominent Q -branch with $\Delta\nu(\text{PR}) = 11.3 \text{ cm}^{-1}$.²⁷ On the other hand, there is little to distinguish a type-A from a type-B band; under conditions of modest resolution, both may be expected to look alike with somewhat poorly defined P -, Q -, and R -branches of roughly equal intensity and $\Delta\nu(\text{PR}) = 9.0 \text{ cm}^{-1}$, in keeping with the approach of the molecule to an oblate symmetric top. Hence, although the i.r. spectrum of gaseous dimethylamidogallane includes some absorptions which display clear signs of partially resolved rotational structure (e.g. those at $1\,907$ and $1\,047 \text{ cm}^{-1}$), this serves only to differentiate between b_{1u} modes, with their pseudo-parallel-type contours, and b_{2u} or b_{3u} modes, with their pseudo-perpendicular-type contours.

GaH₂ Groups. The four stretching vibrations of the terminal GaH_2 groups are readily identified, e.g. by their positions, by the band-contours of the i.r. absorptions associated with the vapour, and by their response to deuteration ($\nu_{\text{H}}/\nu_{\text{D}} \sim \sqrt{2}$). Of the eight GaH_2 bending modes (involving scissoring, wagging, or rocking motions), four are active in Raman scattering and three in i.r. absorption. On the evidence of their positions and response to deuteration, the i.r.-active modes of $[\text{Me}_2\text{NGaH}_2]_2$ are identified with absorptions near 730 , 690 , and 575 cm^{-1} . This includes the absorption of the vapour at 733 cm^{-1} which corresponds presumably to the feature at 743 cm^{-1} ascribed previously to the Ga-N stretching fundamental of the monomeric Me_2NGaH_2 molecule.² Our revised assignment based on the dimer $[\text{Me}_2\text{NGaH}_2]_2$ explains the failure of earlier researchers to detect the corresponding feature of Me_2NGaD_2 .² Similar arguments cause us to assign the Raman scattering near 740 , 730 , 685 , and 540 cm^{-1} to the b_{3g} , a_g , b_{1g} , and b_{2g} bending modes respectively.

NC₂ Groups. The stretching vibrations of the NC_2 groups occur in the range $900\text{--}1\,100 \text{ cm}^{-1}$.²¹⁻²⁵ The assignments proposed in Tables 4 and 5 are consistent with the selection rules, with the limited response to deuteration at gallium, and with the vibrational analyses carried out on other dimethyl-amido-derivatives.^{18,21,22,24-26} The b_{1u} fundamental is most plausible associated with the type-C i.r. absorption of the vapour at $1\,047 \text{ cm}^{-1}$ with $\Delta\nu(\text{PR}) = 10.8 \text{ cm}^{-1}$. Bending modes of the NC_2 groups, expected at wavenumbers $< 400 \text{ cm}^{-1}$, are less easy to identify but are probably responsible for i.r. and Raman bands in the region $200\text{--}300 \text{ cm}^{-1}$.

Ga₂N₂ Ring. The Ga_2N_2 ring possesses four stretching fundamentals, two active in i.r. absorption ($b_{2u} + b_{3u}$) and two in Raman scattering ($a_g + b_{1g}$). These we believe to be responsible for the bands between 460 and 520 cm^{-1} , although features due to GaD_2 bending modes obscure this region in the spectra of $[\text{Me}_2\text{NGaD}_2]_2$. There are no obvious candidates for the two deformation modes of the Ga_2N_2 ring ($a_g + b_{1u}$)

but these occur in all probability at wavenumbers $< 200 \text{ cm}^{-1}$, beyond the threshold of the present measurements.

Table 6 includes the results of product-rule calculations. Where the theoretical and observed product-rule factors, P , can be compared for a given symmetry species, the agreement is reasonable. The comparison is tempered by three factors: (i) the internal modes of the methyl groups have been ignored and so any coupling between these and the skeletal modes must affect $P_{\text{calc.}}$; (ii) some of the skeletal modes have escaped detection; and (iii) the anharmonicity of the vibrations is expected to result in the condition $P_{\text{calc.}} \geq P_{\text{obs.}}$. Indeed this condition has been exploited as a means of adjudicating some of the assignments within a particular symmetry class.

Conclusions

Our principal conclusion is that, contrary to previous indications,² dimethylamidogallane exists predominantly as the dimer $[\text{Me}_2\text{NGaH}_2]_2$ in the vapour phase, as in benzene solution, at ambient temperatures. The vibrational spectra indicate too that the same discrete unit is present in the crystalline solid; more definitive studies of single crystals are now underway.²⁸ Hence it resembles the compound $\text{Me}_2\text{NGaMe}_2$ which is dimeric in the vapour phase, in benzene solution, and probably also in the crystalline state.²⁶ Other compounds with the empirical formula $\text{R}_2\text{NGaR}'_2$ (where R , $\text{R}' = \text{H}$ or alkyl) are reported to be associated in the condensed phases, the tendency to form dimers in solution increasing with the bulk of the substituents.^{19,29}

Analysis of the electron scattering due to the vapour indicates the presence of a square Ga_2N_2 ring [$\text{Ga-N-Ga} = 90.6(0.8)^\circ$] at the centre of the molecule. A similar geometry with angles close to 90° is found for the B_2N_2 rings in $[\text{Me}_2\text{NBX}_2]_2$ ($\text{X} = \text{F}^{14}$ or Cl^{15}), the Al_2N_2 ring in $[\text{Me}_2\text{NAlMe}_2]_2$,¹⁶ and the In_2N_2 ring in $[\text{Me}_2\text{NInMe}_2]_2$.¹⁸ The bond length lies at the short end of the range spanned by measured Ga-N distances ($197\text{--}220 \text{ pm}$).⁵ At $202.7(0.4) \text{ pm}$, it is significantly shorter than the Ga-N distance in $\text{Me}_3\text{N-GaH}_3$ [$212.4(0.7) \text{ pm}$].⁵ Although this may reflect in part the transition from a non-cyclic to a cyclic molecule, the major influence is probably the superior basicity and acidity of the units Me_2N^- and GaH_2^+ respectively; the higher-energy highest occupied molecular orbital of Me_2N^- and the lower-energy lowest unoccupied molecular orbital of GaH_2^+ simply result in a better energy match of the frontier orbitals. The Al-N bonds in $\text{Me}_3\text{N-AlMe}_3$ [$209.9(1.0) \text{ pm}$]³⁰ and $[\text{Me}_2\text{NAlMe}_2]_2$ [$195.7(0.7) \text{ pm}$]¹⁶ show a similar pattern. At $288.1(1.7) \text{ pm}$, the $\text{Ga} \cdots \text{Ga}$ distance in $[\text{Me}_2\text{NGaH}_2]_2$ is significantly longer than twice the covalent radius of gallium (240 pm);³¹ the $\text{Al} \cdots \text{Al}$ distance in $[\text{Me}_2\text{NAlMe}_2]_2$ (280.9 pm)¹⁶ is likewise more than twice the covalent radius of aluminium (260 pm). This contrasts with formally electron-deficient molecules like $\text{Me}_2\text{Al}(\mu\text{-R})_2\text{AlMe}_2$ ($\text{R} = \text{H}^{32}$ or Me^{33}) in which the distance between the heavy atoms is close to twice the appropriate covalent radius. It is likely that non-bonded repulsions between the nitrogen atoms of $[\text{Me}_2\text{NGaH}_2]_2$ or $[\text{Me}_2\text{NAlMe}_2]_2$ have a significant influence on the dimensions of the M_2N_2 ring ($\text{M} = \text{Ga}$ or Al). As expected, the cyclic structure of the skeleton constrains the amplitude of vibration of the Ga-N bonds. Thus, the amplitude shrinks from $6.1(1.1) \text{ pm}$ in $\text{Me}_3\text{N-GaH}_3$ ⁵ to $4.5(0.9) \text{ pm}$ in $[\text{Me}_2\text{NGaH}_2]_2$.

The dimensions of the dimethylamido-group are in line with those of related molecules. Representative C-N bond lengths (in pm) and C-N-C bond angles (in $^\circ$) are as follows: $[\text{Me}_2\text{NGaH}_2]_2$ $146.3(1.3)$, $109.6(1.6)$ [electron diffraction (ED)]; Me_2NH 145.5 , 111.8 (ED);^{34a} Me_2NSiH_3 146.2 , 111.1 (ED);^{34b} $\text{P}(\text{NMe}_2)_3$ 145.8 , 113.5 (ED);^{34c} $\text{Sn}(\text{NMe}_2)_4$ 145.0 , 119 (ED);^{34d} $\text{W}(\text{NMe}_2)_6$ 151.6 , 104.9 [X -ray diffraction (X)];^{34e}

$[\text{Me}_2\text{NBF}_2]_2$ 146.9, 107.9 (X);¹⁴ $[\text{Me}_2\text{NBCl}_2]_2$ 150.5, 108.5 (X);¹⁵ $[\text{Me}_2\text{NAlMe}_2]_2$ 149.4, 108.1 (X);¹⁶ $[\text{Me}_2\text{NInMe}_2]_2$ 147.5, 109.0 (X);¹⁸ $[\text{Be}(\text{NMe}_2)_2]_3$ 146.3, 103.6 (X);^{34f} $[\text{Sn}(\text{NMe}_2)_2]_2$ 147.3, 110.2 (X).^{34g} Despite the fact that some of these compounds contain terminal NMe_2 groups and some bridging NMe_2 groups, the dimensions reveal no obvious pattern correlating with the nature of the ligation.

Acknowledgements

We thank the S.E.R.C. for research grants and the award of a research studentship (to P. L. B.) and Jesus College, Oxford, for the award of a Graduate Scholarship (to P. L. B.).

References

- 1 N. N. Greenwood, 'New Pathways in Inorganic Chemistry,' eds. E. A. V. Ebsworth, A. G. Maddock, and A. G. Sharpe, Cambridge University Press, Cambridge, 1968, p. 37.
- 2 N. N. Greenwood, E. J. F. Ross, and A. Storr, *J. Chem. Soc. A*, 1966, 706.
- 3 A. B. Burg and C. L. Randolph, jun., *J. Am. Chem. Soc.*, 1951, **73**, 953.
- 4 J. K. Ruff and M. F. Hawthorne, *J. Am. Chem. Soc.*, 1960, **82**, 2141.
- 5 P. L. Baxter, A. J. Downs, and D. W. H. Rankin, *J. Chem. Soc., Dalton Trans.*, 1984, 1755.
- 6 N. N. Greenwood, A. Storr, and M. G. H. Wallbridge, *Proc. Chem. Soc.*, 1962, 249; *Inorg. Chem.*, 1963, **2**, 1036.
- 7 J. R. Durig, K. K. Chatterjee, Y. S. Li, M. Jililian, A. J. Zozulin, and J. D. Odom, *J. Chem. Phys.*, 1980, **73**, 21.
- 8 A. H. Cowley, *Polyhedron*, 1984, **3**, 389.
- 9 D. F. Shriver and A. E. Shirk, 'Inorganic Syntheses,' ed. A. G. MacDiarmid, McGraw-Hill, New York, 1977, vol. 17, pp. 42, 45.
- 10 C. M. Huntley, G. S. Laurenson, and D. W. H. Rankin, *J. Chem. Soc., Dalton Trans.*, 1980, 954.
- 11 S. Cradock, J. Koprowski, and D. W. H. Rankin, *J. Mol. Struct.*, 1981, **77**, 113.
- 12 A. S. F. Boyd, G. S. Laurenson, and D. W. H. Rankin, *J. Mol. Struct.*, 1981, **71**, 217.
- 13 L. Schäfer, A. C. Yates, and R. A. Bonham, *J. Chem. Phys.*, 1971, **55**, 3055.
- 14 A. C. Hazell, *J. Chem. Soc. A*, 1966, 1392.
- 15 H. Hess, *Z. Kristallogr., Kristallgeom., Kristallphys., Kristallchem.*, 1963, **118**, 361.
- 16 H. Hess, A. Hinderer, and S. Steinhäuser, *Z. Anorg. Allg. Chem.*, 1970, **377**, 1; G. M. McLaughlin, G. A. Sim, and J. D. Smith, *J. Chem. Soc., Dalton Trans.*, 1972, 2197.
- 17 A. Ahmed, W. Schwarz, and H. Hess, *Acta Crystallogr., Sect. B*, 1977, **33**, 3574.
- 18 K. Mertz, W. Schwarz, B. Eberwein, J. Weidlein, H. Hess, and H. D. Hausen, *Z. Anorg. Allg. Chem.*, 1977, **429**, 99.
- 19 N. N. Greenwood and A. Storr, *J. Chem. Soc.*, 1965, 3426; A. Storr, *J. Chem. Soc. A*, 1968, 2605; A. Storr and A. D. Penland, *ibid.*, 1971, 1237.
- 20 K. Nakamoto, 'Infrared and Raman Spectra of Inorganic and Coordination Compounds,' 3rd edn., Wiley, New York, 1978, p. 145.
- 21 D. C. Bradley, *Adv. Inorg. Chem. Radiochem.*, 1972, **15**, 259 and refs. therein.
- 22 A. Finch, I. J. Hyams, and D. Steele, *J. Mol. Spectrosc.*, 1965, **16**, 103.
- 23 N. B. Colthup, L. H. Daly, and S. E. Wiberley, 'Introduction to Infrared and Raman Spectroscopy,' 2nd edn., Academic Press, New York, 1975, pp. 222–227.
- 24 J. R. Durig and J. M. Casper, *J. Mol. Struct.*, 1971, **10**, 427.
- 25 G. Davidson and S. Phillips, *Spectrochim. Acta, Part A*, 1979, **35**, 141.
- 26 O. T. Beachley, G. E. Coates, and G. Kohnstam, *J. Chem. Soc.*, 1965, 3248.
- 27 W. A. Seth Paul and G. Dijkstra, *Spectrochim. Acta, Part A*, 1967, **23**, 2861; W. A. Seth Paul, *J. Mol. Struct.*, 1969, **3**, 403.
- 28 P. L. Baxter, A. J. Downs, M. J. Goode, and C. K. Prout, unpublished work.
- 29 G. E. Coates, *J. Chem. Soc.*, 1951, 2003.
- 30 G. A. Anderson, F. R. Forgaard, and A. Haaland, *Acta Chem. Scand.*, 1972, **26**, 1947.
- 31 J. E. Huheey, 'Inorganic Chemistry: Principles of Structure and Reactivity,' 3rd edn., Harper and Row, New York, 1983, p. 258.
- 32 A. Almenningen, G. A. Anderson, F. R. Forgaard, and A. Haaland, *Acta Chem. Scand.*, 1972, **26**, 2315.
- 33 A. Almenningen, S. Halvorsen, and A. Haaland, *Acta Chem. Scand.*, 1971, **25**, 1937.
- 34 (a) B. Beagley and T. G. Hewitt, *Trans. Faraday Soc.*, 1968, **64**, 2561; (b) C. Glidewell, D. W. H. Rankin, A. G. Robiette, and G. M. Sheldrick, *J. Mol. Struct.*, 1970, **6**, 231; (c) A. V. Vilkov, L. S. Khaikin, and V. V. Evdokimov, *J. Struct. Chem. (USSR)*, 1972, **13**, 4; (d) L. V. Vilkov, N. A. Tarasenko, and A. K. Prokof'ev, *ibid.*, 1970, **11**, 114; (e) D. C. Bradley, M. H. Chisholm, C. E. Heath, and M. B. Hursthouse, *Chem. Commun.*, 1969, 1261; (f) J. L. Atwood and G. D. Stucky, *J. Am. Chem. Soc.*, 1969, **91**, 4426; (g) M. M. Olmstead and P. P. Power, *Inorg. Chem.*, 1984, **23**, 413.

Received 18th July 1984; Paper 4/1244